RESEARCH ARTICLE

Deposition of ultrasonic nebulized aerosols onto a hydrophilic surface

Kusdianto Kusdianto [a,b,*], Masao Gen [b,d], Mitsuki Wada [b], Sugeng Winardi [a], I. Wuled Lenggoro [b,c*]

[a] Department of Chemical Engineering, Institut Teknologi Sepuluh Nopember (ITS), Kampus ITS Surabaya, 60111, Indonesia
[b] Graduate School of Bio-Applications and Systems Engineering, Tokyo University of Agriculture and Technology, Nakacho 2-24-16, Koganei, Tokyo, 184-8588, Japan
[c] Department of Chemical Engineering, Tokyo University of Agriculture and Technology, Nakacho 2-24-16, Koganei, Tokyo, 184-8588, Japan
[d] Faculty of Frontier Engineering, Institute of Science and Engineering, Kanazawa University, Kakuma-machi, Kanazawa 920-1192, Japan

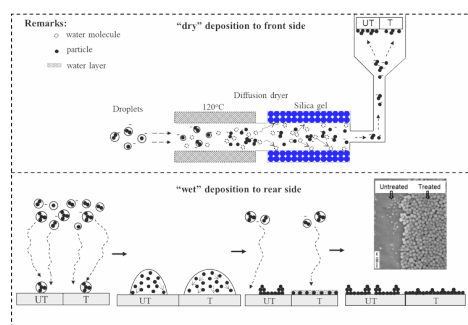* Corresponding author: wuled.@cc.tuat.ac.jp and kusdianto@chem-eng.its.ac.id

Graphical abstract

Abstract

The effect of chemical treatment of a metallic substrate on the deposition of aerosols generated by an ultrasonic nebulizer was investigated. A single substrate with areas having different "level" of hydrophilicity (or hydrophobicity) was used as a model surface. The treated (more hydrophilic) area became more negatively-charged based on a surface electric potential meter. A low-pressure analysis method (electron-microscope image) and ordinary pressure methods (Raman spectroscopy and X-ray fluorescence) analytical results indicated that in comparison with the untreated area, the treated area trapped more particles in the case of the deposition of "wet" aerosols. In the case of the deposition of more "dry" aerosols, the untreated area trapped more particles rather than that of the treated one. The efficiency of particles deposition not only depended on the degree of hydrophilicity (or hydrophobicity) of the surface but also due to the conditions (wet or dry) of incoming aerosols.

Keywords: Charged particles, chemical treatment, electric potential, substrate

INTRODUCTION

Nebulizer system using ultrasonic energy has been widely used for generating droplets with typical size in the micrometer order [1-3]. The generated droplets can be further combined with other methods to produce either dry particles or films, such as via chemical vapor deposition, flame system routes, and thermal decompositions [4-6]. On the other hand, the nebulizer can also be used to fabricate a mesoporous membrane and dense nanolayer coating on the solid substrate [7]. It is reported that the deposition efficiency of particles on the substrate can be enhanced by modifying the substrates either via chemical or physical treatments or combining among them [8, 9].

However, there are few studies considering the effect of substrate treatment on the deposition of particles generated by a nebulizer. Huang et al. investigated the effect of the substrate treated by a physical method using an electron beam to enhance deposition of lead lanthanum titanate on $Pt/TiO_2/Ti/SiO_2/Si$ substrate [5]. The structure of this substrate was fabricated by electron beam evaporation method. Initially, Si wafer was oxidized using oxygen, followed by deposition of titanium layer on silica and then TiO_2 and Pt layer. Another physical treatment method for fabrication of lithiated cobalt oxide film as a cathode for lithium rechargeable batteries using a nebulizer as the droplet generator was also investigated [10]. Furthermore, Xomeritakis et al. also used physical treatment to modify the substrate as a deposition target for fabrication of mesoporous membrane using a nebulizer as a generator [7]. The substrate was made by pressing Al_2O_3 powder and followed by calcination, then polished with abrasive SiC paper.

To the best of our knowledge, there is no study on the relationship between the chemical condition of the surface and the efficiency of aerosol deposition generated by a nebulizer. In our previous study, the deposition of highly positive charged aerosol particles on the aluminium substrate that treated chemically by phosphoric acid had been studied [8]. The treated area showed more hydrophilic than that of the untreated one. The treated area had a higher concentration of the deposited particle than that of the untreated one due to increasing of the electrostatic force between the positively-charged aerosols and the negatively-treated substrate. Inspired by limitation from the previous studies, an ultrasonic nebulizer was used in the present study to generate droplets that having a slightly negative charge. In our hypothesis in this case, a relationship would be expected in the surface treatment, the hydrophilic surface, the surface electric potential and the wet or dry charged aerosols. The objective of this study was to investigate the relationship between the hydrophilicity of the surface and the deposition efficiency of particles generated by ultrasonic nebulizer as "wet" (droplets) and "dry" aerosols.

EXPERIMENTAL

Materials and experimental setup

The starting suspension was prepared by dispersing of SiO_2 colloidal samples (Snowtex, Nissan Chemical Industries, Tokyo) into pure water to make a sample with concentration 0.1 %wt. H_3PO_4 (Wako Pure Chemical Industries, Tokyo) was used for chemical treatment of the substrate. All chemicals were used as received. The substrate was treated by following the same procedure as reported by our previous study [8]. Briefly, an aluminum (Al) sheet with 25 mm in diameter was

treated in the following sequence steps: (i) submerged about half of the substrate into H_3PO_4 solution for making a hydrophilic "patterned" area, (ii) submerged into ultrapure water, and (iii) dried in an oven at 393K for 60 min. The treated and dried substrates were kept in a desiccator before conducting the deposition experiments.

The suspension, SiO_2 0.1 %wt, was homogenized (ultrasonicated, 35 kHz) within 10 min in order to prevent fouling on the wall surface of the container and aggregation before usage. 50 mL of the suspension was subjected into an ultrasonic nebulizer (NE-U17, 1.7 MHz, Omron Healthcare Co. Ltd., Kyoto) to generate droplets. A laboratory-made cooling system, cooling water cycling using a pump, was applied to keep the suspension temperature approximately constant. The temperature of the suspension and the cooling water were measured by using thermocouples connected into a data logger. Two kinds of experimental setups were performed in the present study, namely "wet" and "dry" depositions. In the case of "wet" deposition (Figure 1a), droplets generated by ultrasonic were carried upward by an air stream that was filtered using a HEPA filter toward the substrate. The substrate was positioned perpendicularly from the nozzle of the aerosol

generator. After deposition, the substrate was dried at 80°C for 150 min in a dryer system to produce dry particles prior to the analysis.

In the case of "dry" deposition (Figure 1b), a silica gels-based diffusion dryer was installed in the system in order to remove moisture [11-13]. The droplets were passed through a tube (with an inner diameter of 5 mm and length of 645 mm) that was heated at 120°C. Water molecules after evaporation were adsorbed by silica gels. This system generated drier aerosol particles. The residence time of droplet in the diffusion dryer was estimated about 0.75 s, which was calculated by dividing the volume of its diffusion dryer system to the air flow rate. Furthermore, the time required of single droplet to evaporate was estimated approximately 0.2×10^{-3} s based on an empirical equation [14]. Even though the evaporation rate of a single droplet was less than 1 ms, however, not all droplets might be completely evaporated due to the high concentration of droplets in the specific space. In the experimental setup of the "wet" and "dry" depositions, the front and rear sides of the substrate were used as a target. We did not compare the deposition efficiency of particles in both areas.
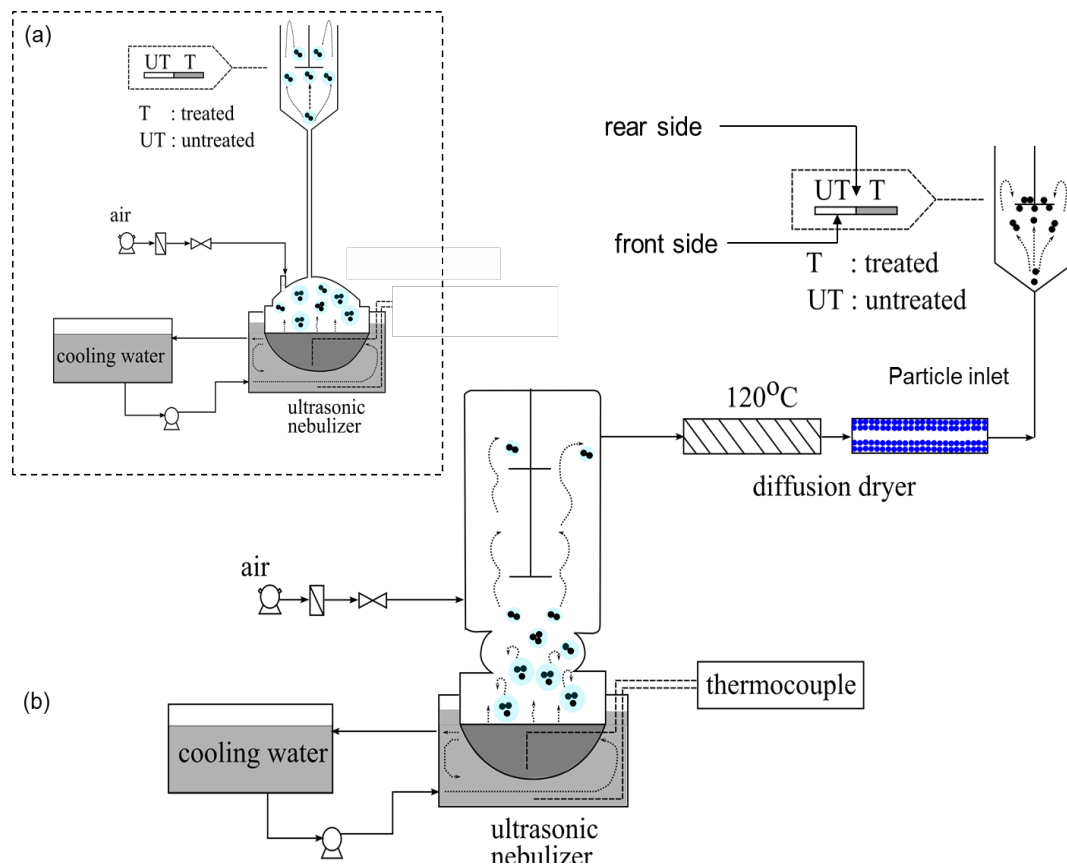

Fig. 1 Schematic illustration of the deposition of ultrasonic nebulized aerosols using "wet" (a) and "dry" (b) deposition onto a hydrophilic surface.

Characterizations

Particle size distribution of the SiO_2 suspension in the liquid phase was measured by dynamic light scattering (HPPS 5001, Malvern Instrument, Worcestershire), while the generated aerosol particle in the gas-phase was measured online by scanning mobility particle sizer (SMPS, TSI 3034, Minnesota). Scanning electron microscope (SEM, JSM 6510, JEOL, Tokyo) was mainly used to observe the morphology of the deposited particles on the surface. Pt-based ion sputtering device (JFC-1100, JEOL), operated at 1.2 kV and 6.5 mA, was used for 1 min three times before observation by SEM. X-ray Fluorescence (XRF, JSX 3100 RII, JEOL), with a tube voltage of 50 kV and 1 mA, was used to investigate the "mass" of Si of the deposited particles under ordinary pressure (1 atm). Another ordinary pressure type analysis, Raman spectroscopy (Nicolet Almega XR Thermo Electron, Barrington) was also used to identify the deposited particles of SiO_2 on the surface.

RESULTS AND DISCUSSION

Deposition of "wet" Aerosol

As reported in our previous study [8], the wettability of the substrate was described by measuring the contact angles of the surface before and after treatments. It was confirmed that the treated surface was more hydrophilic than the untreated one [8]. On the other hand, the surface electric potential of the treated and untreated areas was measured by a non-contact surface potential meter as -590 and -260 mV, respectively. Figure 2 shows the SEM images and the FE-SEM image of the particles deposited on the treated and untreated areas of the rear and front sides in the case of "wet" deposition. Notations of (a)–(e) in Figure 2 are explained in details as depicted in Figure 2(f). Briefly, Figures 2(a) shows the SEM images of deposited particles on the rear side, while Figs. 2 (b) and (c) are the higher magnification from Fig. 2(a) at the untreated and treated areas. The interface between

treated and untreated area in the rear side is observed by FE-SEM as depicted in Fig. 2(d). Moreover, the deposited particles in the untreated and treated areas at the front side is also observed by SEM (see Fig. 2(e)). It is clear that most of the particles were deposited on the treated area compared to the untreated one. Furthermore, the SEM images also showed significantly different structures of the deposited particles between the treated and untreated areas.

On the rear side, the particles were deposited widely in all surfaces, making a homogeneous layer on the treated area, and even few "ring-like structures" were also observed. The aerosol droplets were introduced upward by the carrier gas and formed an aerosol cloud above the substrate where it might gravitationally sink and deposit on the rear side of the substrate [7]. After droplet impacting on the surface, the surface condition was possible to affect the material transfer that occurred on the surface. The droplet spreading on the treated (more hydrophilic) area was easier than that on the untreated area. Spreading of the droplet on the hydrophilic surface might form the water film that could be used for enhancing the hydrophilic interaction [15].
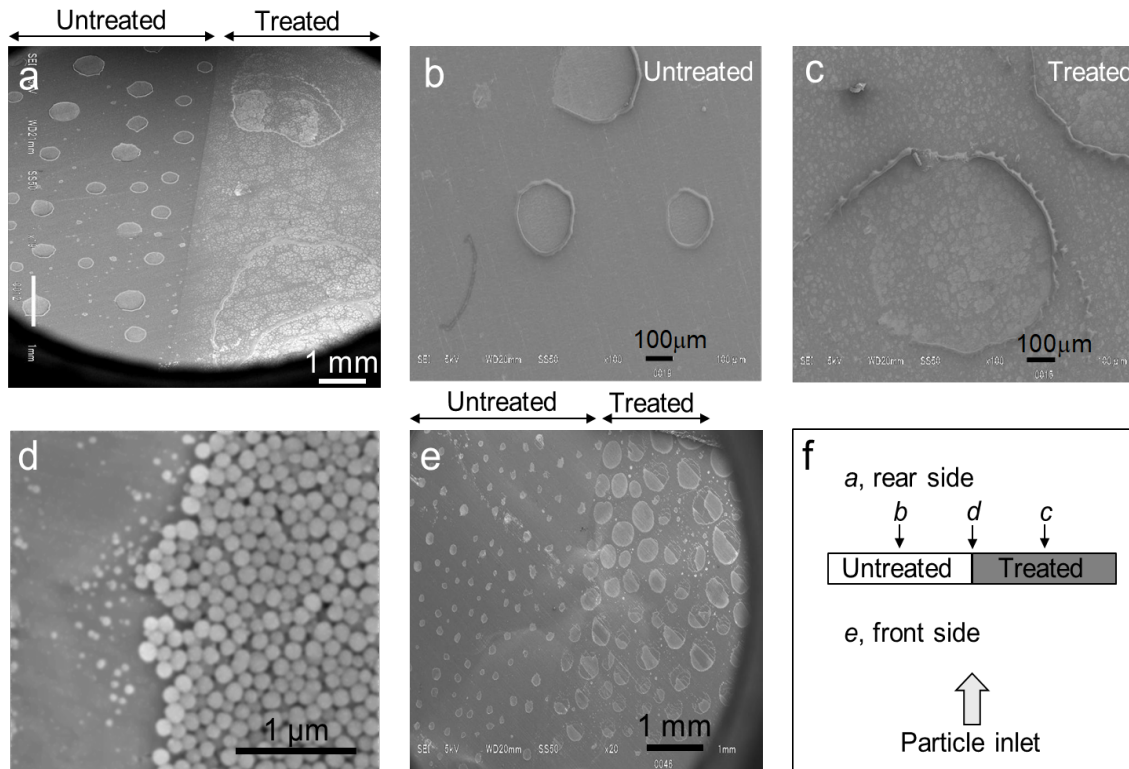

Fig. 2 SEM images of the deposited particles on the substrate in the case of "wet" deposition at: the rear side (a), untreated area at the rear side (b), treated area at the rear side (c), and the front side (e). FE-SEM image at the interface between treated and untreated in the rear side (d).

In contrast, the particle structure on the untreated area mainly showed "ring-like structures" without occupying all surfaces of the untreated area. The same structure could also be found using SiO_2 colloidal suspension on the silicon wafer substrate by ink-jet printing [16], a colloidal polysterene on the substrate [17], and polymer suspension deposited on the polyethylene terephthalate substrate using ultrasonic atomization [18]. The deposited particles formed "ring-like structure" due to flux distribution along the droplet surface that was not uniform in which the evaporation rate was larger at the edge than that of the centre [17]. A "wall" of agglomerated particles was formed in the interface between the treated and untreated areas (Figure 2d). Regarding the "wet" deposition, we also observed the particles deposited in the front side of the substrate as shown in Figure 2(e). The morphology of particles deposited on the treated and untreated areas showed similar structures, however, it has a different size in diameter of the "ring". The treated area has larger size (~ 440 μm) than that of the untreated one (~ 170 μm), attributing to a different "level" of hydrophilicity. As mentioned in previous part that the speed of droplet spreading on the treated (more hydrophilic) area was a higher probability than that on the untreated area, resulting a larger diameter of the "ring" in the hydrophilic surface.

The ordinary pressure analytical method, XRF, was also used to investigate the existence (mass) of chemical element Si of the deposited particles. This method was used to eliminate some problems that might occur in low-pressure analytical technique, such as the possibility of detachment of the deposited particles on the substrate due to a vacuum condition. Figure 3 shows the XRF analysis based on the intensity ratio of Si/Al on the treated and untreated areas in the front and rear sides. The treated area showed a higher value of Si/Al intensity than that of the

untreated one in both sides of the substrate in the case of "wet deposition". It indicated that more particles were deposited on the treated area compared to the untreated one. In contrast with the "wet" aerosol deposition, the untreated area in the "dry" deposition has a higher value than that of the treated one, indicating that more SiO_2 particles were deposited on the untreated areas. It could be ascribed due to the different mechanism of deposition velocities as described in the next part.
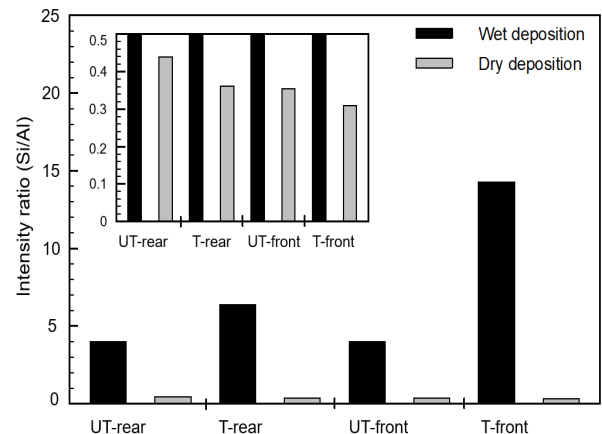

Fig. 3 Ratio between the intensity of SiO_2 (the deposited particles on the substrate) to the intensity of Al substrate in "dry" and "wet" depositions on the treated and untreated areas in front and rear sides of the substrate obtained by the XRF measurement. The enlargement image of intensity ratio for "dry" and "wet" deposition with scale in range of 0 – 0.5 (inset).
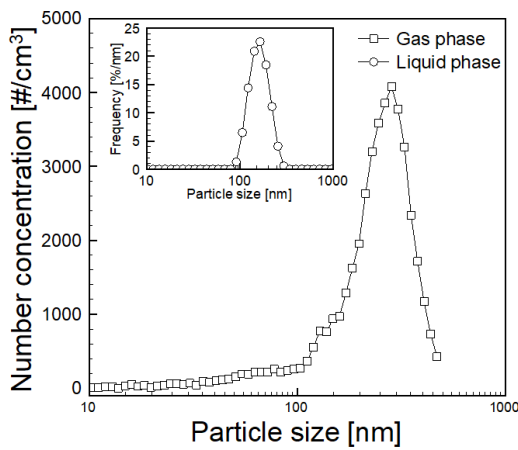
Fig. 4 Particle size distribution in the gas phase measured by SMPS and particle size distribution in the liquid phase measured by DLS (inset).

Deposition of "dry" Aerosol

To investigate the difference between "wet" and "dry" aerosols during their deposition onto a hydrophilic surface, a series of experiment was carried out by installing a silica gel based tubular type diffusion dryer after the generation of droplet aerosols. The size distribution of dried aerosols was measured using a SMPS. Figure 4 shows the particles size distributions of SiO_2 particles in the liquid phase (inset) and after deposition in the dried aerosol. It is clearly observed that the measured average particle size in the gas phase was 240 nm. This value was larger than those of the liquid phase (145 nm), indicating the formation of agglomerated SiO_2 particles. Figure 5 shows SEM images of the particles deposited on the treated and untreated areas in the front and rear sides. The untreated area showed a slightly higher number of the deposited particles in comparison with the treated area. Furthermore, the larger size of the particle structure was shown in the untreated area. These results were consistent with the XRF result shown in the inset of Figure 3, where the untreated area has a higher number of concentrations than that of the treated one, indicating that more SiO_2 particles were deposited on the untreated area.
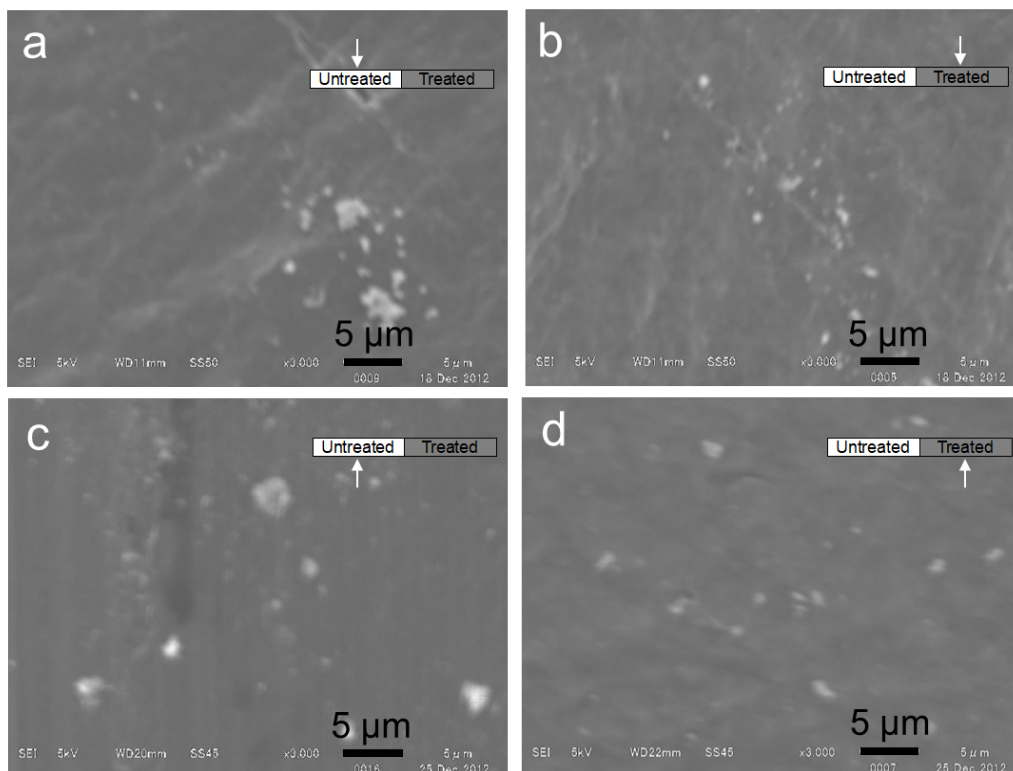

Fig. 5 SEM images of the deposited particles on the treated and untreated areas in "dry" deposition in the rear (a and b) and front (c and d) sides of the substrate.

Another ordinary pressure type analysis method, Raman spectroscopy, was also conducted. Figure 6 shows Raman spectra of SiO_2 particles deposited on the front side including the aluminium substrate before deposition in the case of "dry" deposition.

It is clearly observed that there was no peak at 520 cm^{-1} using aluminium before deposition, however, the strong peak at 520 cm^{-1} was appeared after deposition. The peak at 520 cm^{-1} was attributed to SiO_2. The Raman spectra of the untreated area showed a higher intensity than that of the treated one, indicating that more particles were deposited on the untreated area. This result corresponded to analytical results obtained by SEM and XRF methods which also indicated that the untreated area has higher particles concentration.

Increasing the particles deposited in the untreated area could be ascribed due to the different mechanism of deposition velocities. The deposition velocities near the substrate were considered to predict dynamic of particles from the gas phase onto the solid substrate. These velocities include gravitational, aerodynamic, diffusion and electrostatic effects.
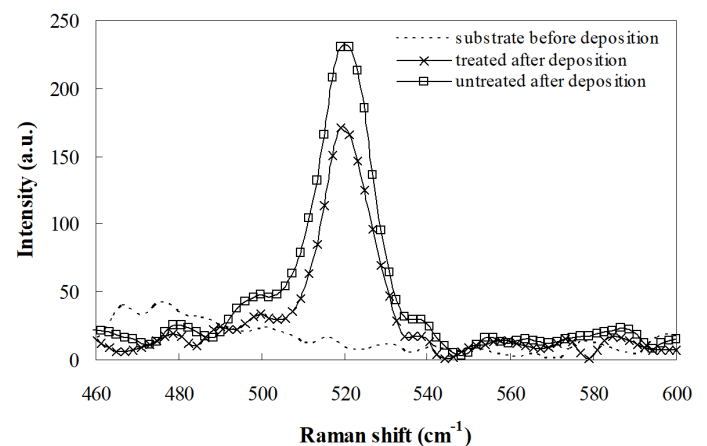

Fig. 6 Raman spectra of particles deposited on the treated and untreated areas in the front side of the substrate, including the aluminium substrate before deposition.

By assuming that the droplet size in "wet" deposition was 5 µm and the solid particle measured by SMPS in "dry" deposition was 0.24 µm, a flow regime in the deposition chamber was numerically calculated with incompressible Navier-Stokes equation and solved by using commercial software (COMSOL Multiphysics 4.3), where the velocity in the vicinity of the substrate was estimated approximately 9.42×10^{-5} m/s. To simplify the equation, evaporation of the droplet was neglected. First, the gravitational deposition velocity, $V_g(d)$ was described in Eq. (1).

$$V_g(d) = mgB \tag{1}$$

where, m, g, and B are the mass of the particle, the gravitational acceleration (9.81 m/s^2), and the mechanical mobility, respectively. The mechanical mobility was expressed as a function of a particle size (d) (Eq. 2).

$$B = \frac{1}{3\pi\mu d} \ (d > 1 \ \mu m) \ or \ \frac{C_c}{3\pi\mu d} \ (d < 1 \ \mu m) \tag{2}$$

where μ and C_c are the viscosity and the Cunningham correction factor, respectively [14]. The mass of a particle was calculated by $\pi d^3\rho_p/6$, where ρ_p is the density of a particle (water = 1000 kg/m^3, silica particle = 2200 kg/m^3). The gravitational deposition velocity calculated by Eq. 1 for particle size $d_d = 5$ µm and $d_s = 0.24$ µm were equal to 7.76×10^{-1} and 6.54×10^{-3} mm/s, respectively.

Aerodynamic deposition velocity, $V_a(d)$ was calculated by

$$V_a(d) = \left[\left(\frac{Stk(d)}{0.6+Stk(d)}\right)^2 + \frac{d}{D}\right]\left(\frac{V}{\pi}\right) \tag{3}$$

where $Stk(d)$ is the Stokes number ($2vmB/D$); D and V are the characteristic length and the flow velocity. Flow velocity at inlet (V) was 1.92×10^{-3} m/s. When length of the substrate was considered to be the characteristic length, D was 0.025 m. Then, the Stokes numbers were calculated as much as $Stk(d_d) = 1.22 \times 10^{-5}$ and $Stk(d_s) = 4.65 \times 10^{-8}$, resulting in $V_a(d_d) = 1.22 \times 10^{-7}$ and $V_a(d_s) = 5.87 \times 10^{-9}$ m/s.

Diffusion velocity, $V_d(d)$ was described by

$$V_d(d) = \frac{kTB}{D}\left\{0.3 + \frac{0.62Re^{0.5}Sc^{\frac{1}{3}}}{\left(1+\frac{0.4}{Sc^{\frac{2}{3}}}\right)}\right\}\left\{1 + \left(\frac{Re}{282000}\right)^{5/8}\right\}^{4/5} \tag{4}$$

where k, T, B, and D are the Boltzmann constant (1.38×10^{-23} J/K), the absolute temperature (293.15 K), the mechanical mobility, and the characteristic length, respectively. Re and Sc are the Reynolds number and the Schmidt number, as described in Eqs. (5) and (6).

$$Re = DV/v \tag{5}$$

$$Sc = v/kTB \tag{6}$$

where v is the kinematic viscosity of air (1.6×10^{-5} m^2/s). The validity of Eq. (4) was ensured when the $ReSc(d)$ was greater than 0.2. The velocity (V) based on numerical simulation was obtained as much as 9.40×10^{-5} m/s. The calculated values of $ReSc(d_d)$ and $ReSc(d_s)$ were more than 0.2. The diffusion velocities were estimated to be $V_d(d_d) = 6.74 \times 10^{-9}$ and $Vd(d_s) = 7.30 \times 10^{-8}$ m/s.

Furthermore, the electrostatic deposition velocity (V_e) could be estimated by using Eq. (7).

$$V_e = qEB \tag{7}$$

where q and E are the charge of a particle and the electric field near the substrate, respectively. However, estimation of the electrostatic force in the "wet" deposition could be neglected. This could be addressed due to the net charge of droplets generated by nebulizer was slightly negative (charge to mass ratio of -0.82 µC/g). Moreover, most of the droplet (98%) measured by an electronic single particle aerodynamic relaxation time were uncharged [19]. Therefore, it was logical to assume that electrostatic force in the case of "wet" deposition could be neglected.

In the summary, the gravitational deposition velocity, aerodynamic velocity, and diffusion velocity calculated using equations (1) – (7) for the "wet" deposition were obtained as much as 7.8×10^{-4}, 1.2×10^{-7}, and 6.7×10^{-9} m/s, respectively. While, the values in the case of "dry" deposition were estimated as 6.6×10^{-6}, 5.9×10^{-9}, and 7.3×10^{-8} m/s, respectively. Regarding the results based on the calculation of deposition velocity, it could be concluded that gravity force was the most dominant during deposition. However, the particle size in the dried aerosol for "dry" deposition was smaller (in submicron size) than the initial sprayed droplet (few micrometer sizes). It should has a higher charge density rather than the corresponding droplet due to water evaporation. This higher charges density might also contribute to the enhancement of the particle deposition, even though the gravity effect was the most dominant according to our calculation. These charges were possible to enhance electrostatic interaction between particles and the substrate, causing more particles deposited on the untreated area.
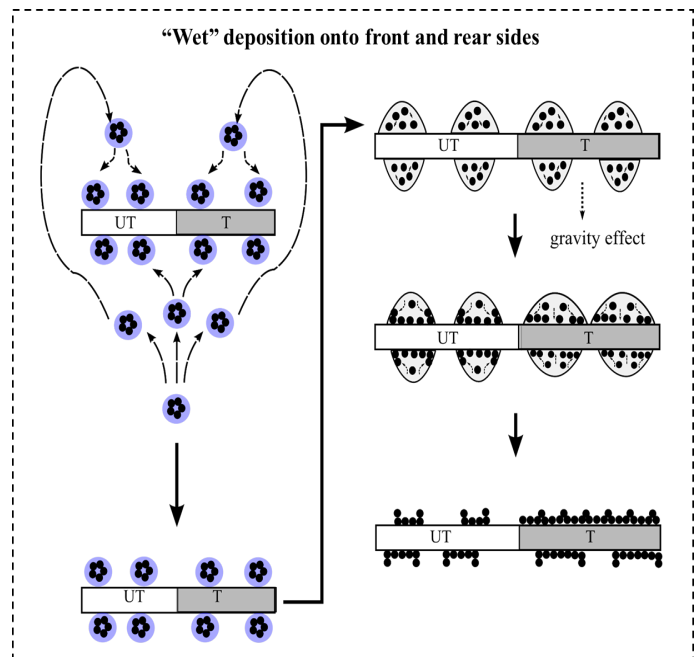

Fig. 7 Illustration of particle deposition mechanism on the treated and untreated area in "wet" deposition.

Mechanism of deposition

There was a different mechanism between the "wet" and "dry" deposition. In the case of "wet" deposition, the treated area has higher number concentration (density) compared to the untreated area. In contrast, the particles deposited on the treated area have less number concentration (density) than that of on the untreated one in the case of "dry" deposition. The different mechanisms in "wet" and "dry" depositions could be explained by illustration as depicted in Figures 7 and 8, respectively. For "wet" deposition (Figure 7), the aerosol droplets were introduced upward by the carrier gas and formed an aerosol cloud above the substrate, where it might gravitationally sink and deposit on the rear side of the substrate [7]. Even the droplet was slightly negatively-charged, however, the gravitation force of bigger droplets might be dominant than electrostatic force. After droplet impacting on the surface, the surface condition was possible to affect the material transfer that occurred on the surface. The droplet spreading on the treated (more hydrophilic) area was a higher probability than that on the untreated area. Spreading of the droplet on the hydrophilic surface might form the water film that could be used for enhancing the hydrophilic interaction [15]. In contrast, after the droplet impacting on the untreated surface (more hydrophobic), and the droplet made a dome shape due to the existence of surface tension. Particles were aggregated in the edge because the evaporation rate was larger at the edge than that of the center [17]. It indicated that the hydrophilicity of the substrate was more dominant for enhancing particle deposition in the "wet" deposition compared to the electrostatic condition of its substrate.
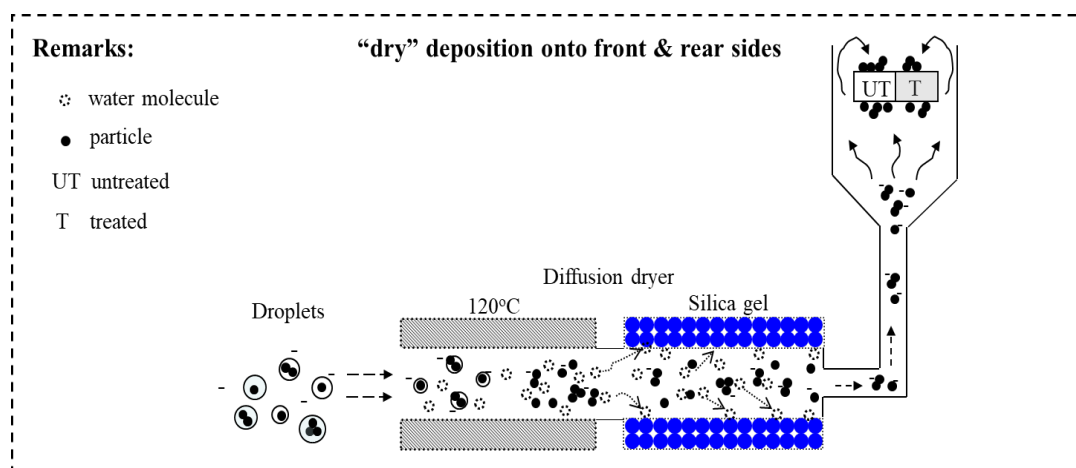
Fig. 8 Illustration of particle deposition mechanism on the treated and untreated area in "dry" deposition.

In the case of "dry" deposition (Figure 8), the particle size of the produced dry aerosol was smaller than the initial sprayed droplet (few micrometer sizes). Even though the droplets have a slightly negative charge [19], however, we believed that these charges might accumulate in the dried particles after solvent evaporation. In our hypothesis, the dried particles should have a higher charge density rather than the corresponding droplet. These higher charges density might also contribute to the enhancement of the particle deposition, even though the gravity effect was still the most dominant according to our calculation. Furthermore, the existence of these charges in the dried particles was possible to enhance electrostatic interaction between particles and the substrate. It then caused the more particles to be deposited on the untreated area. Generally, the particles in the gas stream are transported onto solid surface that influenced by diffusion (Brownian motion for particles smaller than 1000 mm), gravity or settling velocity, inertia force and external force including the electrostatic force [14, 20]. However, the domination for controlling the deposition of particles driven by those forces depends on the strongest force working during deposition.

CONCLUSIONS

The role of the treatment of metal (Al) substrate using phosphoric acid has been investigated in the "wet" and "dry" depositions of aerosols generated by ultrasonic nebulizer. Using a single substrate that has two areas with different levels of hydrophilicity (or hydrophobicity), it was clear that the chemically treated area captured higher particle number concentration than untreated one in the "wet" deposition. In contrast, the treated area collected less particle number concentration in the case of "dry" deposition. Through the current study, it was clear that deposition of "low-charged" aerosols on the substrate depended not only by the substrate condition but also by wettability of incoming aerosols.

ACKNOWLEDGEMENT

REFERENCES

[1]   J. B. Blaisot and J. Yon, *Exp. Fluids* 39 (2005) 977.
[2]   K. Triballier, C. Dumouchel, J. Cousin, *Exp. Fluids* 35 (2003) 347.
[3]   W. N. Wang, A. Purwanto, I. W. Lenggoro, K. Okuyama, H. Chang, H. D. Jang, *Ind. Eng. Chem. Res.* 47 (2008) 1650.
[4]   G. Gritzner, A. Buckuliakova, G. Plesch, K. Przybylski, M. Mair, *Phys. C* 304 (1998) 179.
[5]   C. S. Huang, J. S. Chen, C. H. Lee, *J. Mater. Sci.* 34 (1999) 727.
[6]   C. H. Lee, D. W. Kim, *J. Ceram. Process. Res.* 13 (2012) S377.
[7]   G. Xomeritakis, C. M. Braunbarth, B. Smarsly, N. Liu, R. Kohn, Z. Klipowicz, C. J. Brinker, *Micropor. Mesopor. Mater.* 66 (2003) 91.
[8]   K. Kusdianto, M. Gen, I. W. Lenggoro, *J. Aerosol Sci.* 78 (2014) 83.
[9]   K. Kusdianto, M.N. Naim, K. Sasaki, I. W. *Colloids Surf. A: Physicochem. Eng. Aspects* 459 (2014) 142.
[10]   K. W. Kim, S. I. Woo, K. H. Choi, K. S. Han, Y. J. Park, *Solid State Ion.* 159 (2003) 25.
[11]   B. Han, N. Hudda, Z. Ning, C. Sioutas, *J. Aerosol Sci.* 39 (2008) 770.
[12]   J. H. Jung, G. B. Hwang, J. E. Lee, G. N. Bae, *Langmuir* 27 (2011) 10256.
[13]   T. Oyabu, A. Ogami, Y. Morimoto, M. Shimada, W. Lenggoro, K. Okuyama, I. Tanaka, *Inhal. Toxicol.* 19 (2007) 55.
[14]   W. C. Hinds, *Aerosol technology: properties, behavior, and measurement of airborne particle*, John Wiley & Sons, Inc., (1999) (pp. 278-297).
[15]   M. N. Naim, N. F. Abu Bakar, M. Iijima, H. Kamiya, I. W. Lenggoro, *Jpn. J. Appl. Phys.* 49 (2010) 06GH17.
[16]   J. Park, J. Moon, *Langmuir* 22 (2006) 3506.
[17]   R. D. Deegan, O. Bakajin, T. F. Dupont, G. Huber, S. R. Nagel, T. A. Witten, *Phys. Rev. E* 62 (2000) 756.
[18]   M. Darmawan, K. Jeon, J. M. Ju, Y. Yamagata, D. Byun, Sens. *Actuators A-Phys.* 205 (2014) 177.
[19]   M. Ali, R. N. Reddy, M. K. Mazumder, *J. Electrost.* 66 (2008) 401.
[20]   J. H. Seinfeld, S. N. Pandis, *Atmospheric chemistry and Physics*, John Wiley & Sons, Inc., (1998) (pp.465-474).